

# Dynamic Exploration-Exploitation Trade-Off in Active Learning

## Regression with Bayesian Hierarchical Modeling

Upala Junaida Islam<sup>a,\*</sup>, Kamran Paynabar<sup>b</sup>, George Runger<sup>a</sup>, and Ashif Sikandar Iquebal<sup>a,\*</sup>

<sup>a</sup>School of Computing and Augmented Intelligence, Arizona State University, USA

<sup>b</sup>H. Milton Stewart School of Industrial & Systems Engineering, Georgia Institute of Technology, USA

### Abstract

Active learning provides a framework to adaptively sample the most informative experiments towards learning an unknown black-box function. Various approaches of active learning have been proposed in the literature, however, they either focus on exploration or exploitation in the design space. Methods that do consider exploration-exploitation simultaneously employ fixed or ad-hoc measures to control the trade-off that may not be optimal. In this paper, we develop a Bayesian hierarchical approach to dynamically balance the exploration-exploitation trade-off as more data points are queried. We subsequently formulate an approximate Bayesian computation approach based on the linear dependence of data samples in the feature space to sample from the posterior distribution of the trade-off parameter obtained from the Bayesian hierarchical model. Simulated and real-world examples show the proposed approach achieves at least 6% and 11% average improvement when compared to pure exploration and exploitation strategies respectively. More importantly, we note that by optimally balancing the trade-off between exploration and exploitation, our approach performs better or at least as well as either pure exploration or pure exploitation.

*Keywords:* Active learning regression; Exploration-exploitation trade-off; Bayesian hierarchical model; Approximate Bayesian Computation.

## 1 Introduction

The past decade has witnessed the widespread adoption of machine learning techniques in the design and discovery of novel materials [1], monitoring and control of advanced manufacturing [2], and decision-making in healthcare [3]. However, a majority of the success stories of machine

---

\*Corresponding authors: uislam@asu.edu, aiquebal@asu.edu

learning methods in these domains have been limited to fitting large experimental and simulated datasets [4]. With rising concerns about resource availability and increasing costs of conducting physical experiments and obtaining labeled datasets, there is a need to develop methodologies that can guide experimental efforts towards gathering the most informative experiments.

Active learning provides a framework to address these challenges by allowing the learning algorithm to adaptively select the experiments that are the most informative in learning a concept (a classification or a regression model), thereby reducing the cost of obtaining labeled data [5]. Here, the informativeness of a data sample is usually assessed via an acquisition function. Following the seminal work of Angluin on “Queries and Concept Learning” [6] where the acquisition function was a majority vote among a set of candidate hypotheses, several acquisition functions were introduced that are based on entropy [7], prediction uncertainty [8], etc. These acquisition functions have been successfully implemented in both classification problems [9] and regression problems [10], albeit the primary focus has been on classification. When the target concept is an unknown black-box function, another application of active learning that became popular is “Bayesian optimization” which instead of finding the best fit, seeks the extremum of the function [11]. While finding the optimum of a function seems crucial, learning the underlying black-box function is critical to understanding the effect of design variables on the response and subsequently making predictions for new designs. In this work, we focus specifically on active learning for regression problems where the target concept is an unknown black-box function.

Active learning reduces the overall cost of obtaining labeled data by sequentially querying the most informative ones. However, recent studies have shown that they may have exploration or exploitation bias [12]. For instance, a greedy sampling-based acquisition function proposed in [13] (see Eq. (11)), tends to sample the data points uniformly in the unexplored search space and therefore favors exploration, irrespective of the underlying target concept. An example of this is shown in Figure 4(a). In contrast, a Query-by-Committee (QBC) approach for active learning [14] tends to exploit the search space in the neighborhood where the target concept violates the continuity and, in some cases, uniform continuity assumptions. An example is shown in Figure 4(b). Another approach within the Bayesian Optimization framework, expected improvement [15] often gets stuck in local optima due to exploitation bias even though the primary focus is global optimization of the black-box function. Several improvements have been proposed to overcome this bias [16].

This raises the classic, albeit an important question: how can we encode exploration-exploitation trade-off into the learning process when the target concept is an unknown black-box function. Based on our survey of the literature, we note two prominent schools of thought. The first is based on constructing new acquisition functions or appropriate modifications thereof to balance exploration and exploitation. For example, hierarchical expected improvement (HEI) [16] were introduced in attempt of a non-myopic search for Bayesian optimization. But the most commonly investigated approach is based on optimizing the sum of two acquisition functions using a trade-off parameter controlling the amount of exploration and exploitation [12] and is given as,

$$\mathbf{x}^* = \underset{\mathbf{x}}{\operatorname{argmax}} (\eta \mathcal{F}_1(\mathbf{x}) + (1 - \eta) \mathcal{F}_2(\mathbf{x})) \quad (1)$$

Here,  $\eta \in [0, 1]$  is a parameter controlling the trade-off between  $\mathcal{F}_1(\cdot)$  and  $\mathcal{F}_2(\cdot)$ , the objective functions corresponding to exploration and exploitation respectively, obtained from two separate acquisition functions, and  $\mathbf{x}^*$  is the optimal data to query according to the strategy. Nonetheless, the challenge with both of these approaches is that  $\eta$  is unknown and needs to be estimated during the learning process. Since it is difficult to estimate  $\eta$  without observing future data points, existing approaches have relied on trial and error [17] or predefined ad-hoc measures depending on the number of queried samples [18]. In the reinforcement learning literature, exploration-exploitation trade-off has been extensively studied. However, unlike active learning, the agent in reinforcement learning is only concerned with maximizing the long-term reward by finding an optimal sequence of actions via exploration-exploitation. Hence, we observe the approaches such as exploitation with uncertainty (upper confidence bound or UCB [19]), exploitation with a fixed degree of exploration (greedy epsilon [20]), and exploitation with decreasing degree of exploration (decaying greedy epsilon [20]) to be more prominent in reinforcement learning literature. In active learning, we are concerned with maximizing the rewards over a finite (often very small) number of experiments that we can perform. The active learner, therefore, needs to iteratively update the trade-off parameter as new data samples are queried.

The variability of queried samples within and between sampling stages creates a hierarchical structure of problem where the levels of the hierarchy originates from the variability in the queried sample as well as from sampling at different stages. It allows us to use a Bayesian hierarchical or

multilevel modeling where the dependency of parameters related by the hierarchy is reflected in a joint probability model, and the posterior density and uncertainty quantification of the parameters are obtained via Bayesian inference [21]. In case of the absence of any closed-form expressions for the posterior distribution, a sampling-based Markov chain Monte Carlo (MCMC) method can be used to obtain the marginal posterior distributions [22].

To this end, we present an active learning approach for learning an unknown black-box function by balancing the exploration-exploitation trade-off. In particular, we develop a Bayesian hierarchical model to iteratively update the exploration-exploitation trade-off as data points are queried sequentially to rapidly minimize the generalization error. By imposing a hierarchical structure, we account for the variability in  $\eta$  arising from within each query iteration as well as across subsequent queries. We then present an Approximate Bayesian Computation (ABC) approach along with Metropolis within Gibbs algorithm to sample from the posterior distribution of  $\eta$ . We subscribe to Gaussian Process Regression to obtain the best fit for the underlying black-box function. The proposed methodology is generalizable and not contingent on the choice of exploration and exploitation or the choice of the regression function. We evaluate the efficacy of the proposed active learning methodology on six simulated case studies and one real-world example in materials discovery.

The rest of the paper is organized as follows, Section 2 presents a brief relevant literature review. Section 3.1 unfolds the Bayesian hierarchical model for estimating the trade-off parameter to balance exploration and exploitation. Section 3.2 explains the Gaussian process regression methodology we employed active learning with. Exploration and exploitation approaches adopted in this work are presented in Section 3.3 followed by trade-off strategies commonly used in the literature summarized in Section 3.4. Experimental setup and results from simulation and real-world experiments are presented in Section 4. The paper is concluded in Section 5.

## 2 Literature Review

The idea of carefully choosing experiments or data is not new. Mathematicians and statisticians have employed different methods of experimental designs to estimate parametric and non-parametric models after the notion of design of experiments (DOE) was introduced [23]. The application of sequential experimental design can be traced back to the 1960s [24] where the selection of

experiment to conduct in a statistical decision problem is made sequentially after each observation [25]. The concept of sequential experimental design transpired from the field of statistics to that of machine learning in the form of active learning [26]. In this section, we present a brief review of active learning for regression problems and discuss the recent developments on the exploration-exploitation trade-off. Excellent reviews of active learning literature may be found in [5].

Two of the pioneering and popular works of active learning in regression problems are Active Learning - Mackay (ALM) based on maximizing the expected information gain [10] and Active Learning - Cohn (ALC) based on minimizing the generalization error [8]. Mackay defined the information gain as the change of Shannon's entropy [27] before and after labeling data. Entropy has also been used as a measure for querying data in classification problems within the framework of "uncertainty sampling" [9]. Mackay also demonstrated that the change of entropy at a queried data point depends precisely on its variance. Higher variance indicates higher uncertainty at that location and is expected to contribute more to the learner's current knowledge. For many interpolation models including Gaussian Process regression (GPR), this leads to slightly more concentrated data collection at the edges of the input space [10]. It also allows the model to sample more data near the outliers since they are likely to have higher uncertainty [28] inevitably increasing the generalization error. Cohn et al. [8], on the other hand, demonstrated that the expected generalization error is composed of data noise, model bias, and variance. Data noise is independent of the model, and model bias is invariant given a fixed model. Thus the criteria for querying data is again simplified to the reduction of the total variance. Meka et al. [29] extended this strategy by adding a regularizing term to integrate the information of both evaluated and unevaluated data.

A more theoretically-motivated data selection strategy is the Query-by-Committee (QBC) algorithm [30]. QBC maintains a committee of hypotheses that are simultaneously trained on the labeled data. The data that maximizes the disagreement between the committee members is deemed the most informative. This disagreement has been defined for classification problems via measures such as vote entropy [31], and average Kullback-Leibler (KL) divergence between a particular committee member and the rest of the committee [32]. QBC was first implemented in regression by Krogh and Helseby [33] who defined disagreement as the difference in the predicted variance of the committee members from each other. RayChaudhui and Hamey [34] formed a committee of members with the same structure of regression model, but trained them on a different subset of

data, and defined the disagreement as the predicted variance. This raises the dilemma of selecting subsets which were subsequently tackled using concepts like “query by bagging” and “query by boosting” [35]. A variation of QBC, Expected Gradient Length (EGL) was proposed for classification problems [36] but was implemented in a regression setting under the name of Expected Model Change Maximization (EMCM) [37]. Like QBC, this acquisition function builds a committee of models using samples of the labeled dataset. But unlike QBC, the unlabeled data is scored based on the disagreement between the predicted response and is based on the entire training dataset and the aggregated response of the committee [38]. Inspired by the Stochastic Gradient Descent (SGD) update rule, Cai et al. [37] estimated the model change using the gradient of the error with respect to candidate data and found it to outperform QBC on several datasets. The negative effect of selecting an outlier can be relieved by sampling data that can maximize the change of the model again. But the number of outliers needs to be very small in practice for this strategy to perform well.

QBC and EMCM both require a repeated generation of predictive models increasing the processing time. O’Neil et al. [38] compared them with a few model-free strategies that select data based on geometric point of view only. These model-free acquisition functions include selecting the unlabeled data based on density, or diversity, and their combination in an acquisition function named Exploration Guided Active Learning (EGAL) for classification problems [39]. Density-based acquisition function selects the point closest to the existing training set in the input space, and the diversity-based acquisition function selects the one least similar to (i.e. farthest from) the training set in the input space. EGAL nominates candidate points high in diversity and then selects the one that has the maximum density. Results from O’Neal et al. [38] indicated that the integral properties of the dataset, such as its geometry, can be promising candidates for active learning strategies. A similar diversity-based algorithm named Greedy sampling (GS) was introduced as a passive sampling strategy where data were sampled based on only a geometric characteristics in the feature space and independent of the regression model [40]. More recently, GS was adapted for active learning by incorporating the response information and was referred to as improved Greedy Sampling (iGS) [13] which ensures diversity in both input and output space and explores the entire region in a near-uniform fashion. In a regression setting, regional exploitation strategy has not been defined yet where data collection would be higher at uncertain regions showing discontinuity or irregularities.

The concept of exploration-exploitation trade-off has been studied in several machine learning algorithms. However, switching between exploration and exploitation based on their performance at each iteration [41], a random probabilistic measure [18], or combining them in a predefined ratio [12] does not depend on the selected acquisition function from the previous action. Combining the two acquisition functions based on cross-validation or trial-and-error [17] requires labeling more data than necessary, hence diminishing the effectiveness of active learning since the main objective is to decrease the required number of labeled data without compromising the regression accuracy. Literature has designed the exploration and exploitation strategies differently according to the objective and the nature of the problem. Holub et al. [42] used maximum entropy and mutual information as the strategy to explore and exploit search space respectively. In active learning literature of classification, researches have used Kernel Farthest First (KFF) [43], distance and similarity-based metrics [12] for exploration, and subscribed to uncertainty and redundancy [44] and a few other strategies to exploit near the current decision boundary. While the reviewed literature on active learning mainly focuses on classification and Bayesian optimization, this study intends to advance the research on the less explored regression-based problems, and find a structured algorithm to dynamically update the combination of designated active learning strategies for exploration and exploitation throughout the learning process.

### 3 Methodology

In this section, we briefly present the general schema of active learning along with the models and strategies we employ in this study. In the generic problem of active learning, we consider that among the possible collection of all design points,  $X = \{\mathbf{x}_1, \mathbf{x}_2, \dots\}$ , and their corresponding responses,  $\mathbf{y} = \{y_1, y_2, \dots\}$ , the actively growing set of observed (i.e., labeled) data  $\mathcal{D}^N = \{(\mathbf{x}_{o_i}, y_{o_i})\}_{i=1}^N$  is accessed by the underlying model where  $\mathbf{x}_{o_i} \in \mathbb{R}^d$  are the sampled queries so far, and  $y_{o_i} \in \mathbb{R}$  is the corresponding output response. The objective of active learning in a regression setting is to select the next sample  $\mathbf{x}_{o_{N+1}}$  from the search space  $\mathcal{S}$  which will be the most informative towards learning the unknown black-box function  $f(\mathbf{x})$  given the current knowledge. The response  $y_{o_{N+1}}$  is obtained via simulation or physical experiments. By actively selecting the data to learn from, it can rapidly reduce the generalization error which is the prediction error of the algorithm at the data unobserved

so far. The process is iterated until stopping criteria e.g., the maximum number of labeled data, or predicted change, have been satisfied. See Figure 1 for a flow chart of the active learning approach.

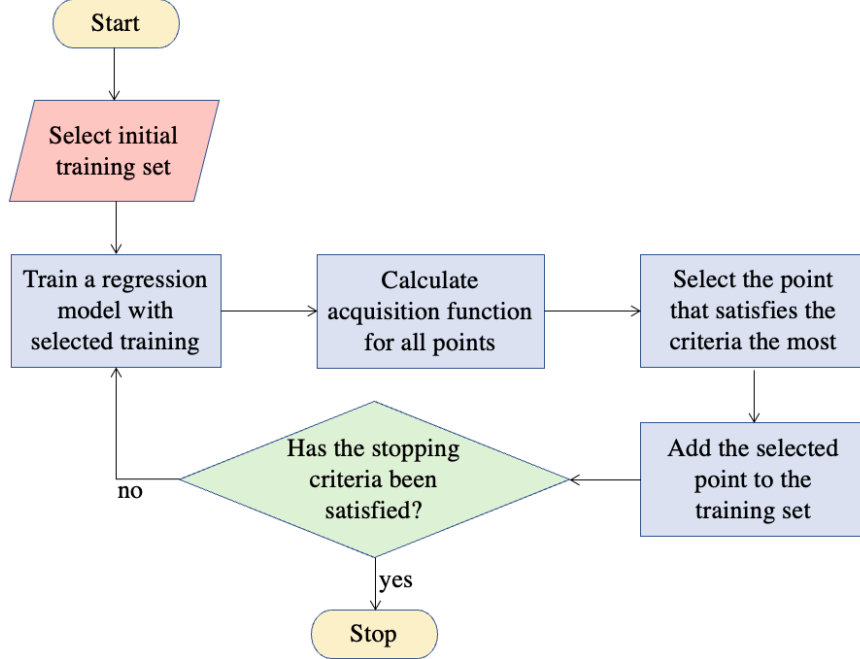


Figure 1: General schema of an active learner

### 3.1 ***Exploration-exploitation trade-off***

In machine learning, exploration refers to generating novel information in the search space while exploitation focuses on improving some decisions (e.g., maximizing reward) based on the available information. Although this is a generally accepted definition of exploration and exploitation [45], its usage varies depending on the context. Particularly, in the regression setting, exploration refers to sampling data from the unobserved regions in the search space to gather more (potentially novel) information about the black-box function, such as local minima/maxima. In contrast, exploitation aims at accurately capturing the black-box function in the regions where it is highly unpredictable and has a sharp change or discontinuities. As mentioned in the foregoing, it is possible to encode exploration and exploitation separately in an acquisition function [39], however, it is challenging to dynamically balance between the two [46]. We consider a general framework for sampling data points that maximizes a linear combination of acquisition functions aimed at simultaneous exploration and

exploitation as presented in Eq. (1). The next data is sampled through pure exploitation when  $\eta = 0$ , and pure exploration when  $\eta = 1$ . By increasing  $\eta$  from 0 to 1, the degree of exploration increases in the constructed acquisition function.

To estimate  $\eta$  dynamically, we consider two levels of variability. First is the variability in queried samples at each sampling stage that emerges from the noise and measurement errors in  $y$ . The second level of variability is associated with the dynamic nature of  $\eta$  from one sampling stage to the next due to the nature of the unknown black-box function (e.g., jumps or discontinuities). This bi-level nature of variability motivates the need for a hierarchical model. A Bayesian hierarchical model allows us to capture this hierarchy while simultaneously encoding the uncertainty at each of the levels. The trade-off parameter  $\eta_j$  captures the first level of variability at sampling stage  $j$  given the set of hyper-parameters  $\boldsymbol{\theta}$ . We model  $\{\eta_j|\boldsymbol{\theta}_j\} \stackrel{iid}{\sim} p(\eta|\boldsymbol{\theta}_j)$ . Here, the conditional independence of  $\{\eta_j|\boldsymbol{\theta}_j\}$  tells us that the trade-off parameters at one sampling stage are exchangeable (de Finetti's theorem [47]), but not independent. To capture the variability in  $\eta$  across multiple sampling stages, we model  $\{\boldsymbol{\theta}_j|\boldsymbol{\psi}\} \stackrel{iid}{\sim} p(\boldsymbol{\theta}|\boldsymbol{\psi})$  where  $\boldsymbol{\psi}$  is another set of hyper-parameters fixed from *a priori* assumptions. De Finetti's theorem from this conditional independence shows that the trade-off parameters at subsequent sampling stages are exchangeable as well. Indeed, this aligns with our assumption that the trade-off parameter at any sampling stage is not completely independent of the previous actions (exploration or exploitation). A schematic of this hierarchy presented in Figure 2 shows how a fixed set of hyper-parameters  $\boldsymbol{\psi} = \{a, b\}$  guides  $\boldsymbol{\theta} = \{\alpha, \beta\}$ , which in turn guides  $\eta$  and subsequently helps in electing the data to query. In the next two subsections, we discuss the prior and the sampling distributions employed in this study.

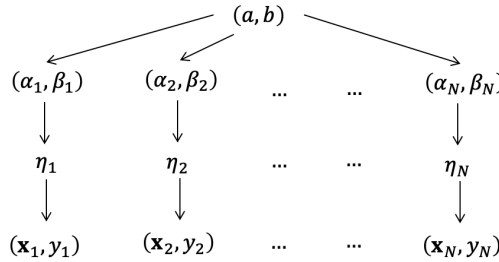


Figure 2: Hierarchical structure of the model

### 3.1.1 Prior distribution

Towards optimally estimating  $\eta$  using a Bayesian hierarchical framework, we begin by considering a prior distribution based on our current knowledge that it lies between 0 (pure exploitation) and 1 (pure exploration). With this prior knowledge, we let  $\eta$  follow a beta distribution in the form of  $\eta \sim \text{Beta}(\alpha, \beta)$  with hyperparameters  $\alpha$  and  $\beta$ . The combined selection of the hyperparameters  $\alpha$  and  $\beta$  defines the shape of the prior distribution of  $\eta$  as observed in Figure 3. A larger value of  $\alpha$  shifts the bulk of the probability towards 1 and emphasizes exploration only (e.g.,  $\alpha = 5, \beta = 0.1$ ), whereas an increase in  $\beta$  moves the distributions towards 0 and encourages exploitation (e.g.,  $\alpha = 0.1, \beta = 5$ ).  $\alpha = \beta < 1$  creates a U-shape distribution with maximum probability near 0 and 1 imposing a similar higher probability on both exploration and exploitation (e.g.,  $\alpha = \beta = 0.1$ ). On the other hand,  $\alpha = \beta > 1$  generates a bell-shape distribution with the maximum probability at the middle ( $\eta = 0.5$ ) imposing a lower probability on pure exploration and exploitation, and a higher probability on a mixture of them (e.g.,  $\alpha = \beta = 0.5$ ). Finally,  $\alpha = \beta = 1$  creates a uniform distribution with equal probability everywhere and is indifferent towards the selection of  $\eta$ .

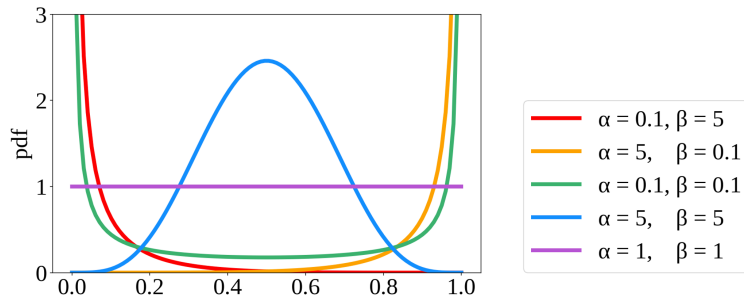


Figure 3: Probability density function for the beta distribution

Based on extensive simulations, we note that changing the range of  $\alpha$  and  $\beta$  beyond the interval of  $a = 0.1$  and  $b = 5.0$  has no significant impact on the exploration-exploitation trade-off. Without any information about the nature of the black-box function, we impose a uniform prior distribution in the form of  $\alpha, \beta \sim \text{uniform}(0.1, 5.0)$ .

### 3.1.2 Posterior and sampling distribution

The joint posterior distribution of  $\eta$  and its hyper-parameters is,

$$p(\eta, \alpha, \beta | \mathbf{y}, X) \propto p(\alpha)p(\beta)p(\eta|\alpha, \beta)p(\mathbf{y}, X|\eta) \quad (2)$$

where  $\{(X, \mathbf{y})\}$  represents the collection of both labeled and unlabeled data. In Eq. (2),  $p(\mathbf{y}, X|\eta)$  is the likelihood of  $\eta$  denoted by  $\mathcal{L}(\eta; \mathbf{y}, X)$  and  $p(\eta|\alpha, \beta)$  is the prior. The hyperprior  $p(\alpha)p(\beta) = p(\alpha|a)p(\beta|b)$  due to the Independence of  $\alpha$  and  $\beta$  as well as *a priori* selection of  $a, b$ . Since the nonstandard joint posterior distribution in Eq. (2) is not available in the closed form, the unknown parameters can be approximated by sampling from their respective full conditional distributions using Gibbs sampling. The individual full-conditional distribution of  $\alpha, \beta, \eta$  can be factorized as

$$\begin{aligned} p(\alpha|\beta, \eta) &\propto p(\alpha)p(\eta|\alpha, \beta) \\ p(\beta|\alpha, \eta) &\propto p(\beta)p(\eta|\alpha, \beta) \\ p(\eta|\alpha, \beta, \mathbf{y}, X) &\propto p(\eta|\alpha, \beta)p(\mathbf{y}, X|\eta) \end{aligned} \quad (3)$$

The Gibbs sampler proceeds by iteratively constructing a dependent sequence of parameter values whose distribution converges to the target joint posterior distribution [48]. But none of the full-conditional distributions in Eq.(3) have a closed-form. Moreover, the likelihood of  $\eta$  is intractable unlike that of  $\alpha$  and  $\beta$  since the generation of new data from observed  $\eta$  does not follow any known distribution. In the absence of a tractable likelihood, we subscribe to Approximate Bayesian Computation (ABC) which has been used in numerous previous applications where it is computationally expensive or infeasible to evaluate the likelihood [49]. Originally introduced in [50], the traditional ABC algorithm, also known as ABC rejection sampler, follows a two step procedure to sample from the posterior distribution. First, it draws samples of the unknown parameter value from its prior distribution. Second, the sampled parameter values are accepted based on the similarity between the data simulated under some model specified by the sampled parameter values and the observed data, or between the summary statistics thereof. In other words, ABC uses summary statistics to filter samples that do not agree with the observed data. Though efficient in simple probability models, ABC rejection is limited in complex ones where the posterior is greatly differ-

ent from the prior since it involves sampling from the prior [51]. Several different computational methods have been presented in the last two decades in order to overcome this limitation of of ABC inference, among which ABC-MCMC and its variants have been widely used and accepted [51]. The ABC-MCMC algorithm combines ABC with Metropolis-Hastings or Metropolis algorithm for iterative approximate Bayesian computation. We will first discuss the Metropolis sampling followed by the incorporation of ABC and summary statistics into the employed methodology. Metropolis sampling is a simplified form of the Metropolis-Hastings sampling algorithm. It proposes a symmetric proposal distribution  $J(\theta|\theta_{old})$  for the parameter vector  $\theta$  given the most recent accepted sample  $\theta_{old}$  at each sampling stage. Each proposed sample is either accepted or rejected depending on an acceptance ratio computed from the prior and likelihood of the proposed and old samples. ABC-MCMC algorithm shadows the steps of a typical Metropolis algorithm. The initial sample is drawn from the prior, and the next ones are sampled from a proposal distribution centered at the most recently accepted sample. But the acceptance ratio constructed by ABC uses summary statistics, therefore replacing the likelihood ratio like in regular Metropolis algorithm.

To avoid the difficulty regarding closed-form full conditionals, we use the Metropolis-within-Gibbs sampler. While used within Gibbs sampler, the Metropolis algorithm updates the parameters  $\{\alpha, \beta, \eta\}$  individually instead of updating the entire vector of parameters,  $\boldsymbol{\theta} = \{\alpha, \beta, \eta\}$  [52]. We initiate the sampler with  $\boldsymbol{\theta}^{(0)} = \{\alpha^{(0)}, \beta^{(0)}, \eta^{(0)}\}$ , and generate a dependent sequence of the parameter vector,  $\{\boldsymbol{\theta}^{(1)}, \boldsymbol{\theta}^{(2)}, \dots, \boldsymbol{\theta}^{(s)}\}$  using Metropolis-within-Gibbs. Given a current state of the parameters  $\boldsymbol{\theta}^{(s)} = \{\alpha^{(s)}, \beta^{(s)}, \eta^{(s)}\}$ , the next state of the parameter vector is generated as follows,

- Sample  $\alpha^{(s+1)} \sim p(\alpha|\beta^{(s)}, \eta^{(s)})$ : We use Metropolis algorithm to sample  $\alpha^{(s+1)}$  till it converges. Metropolis sampling proposes a symmetric distribution centered on the most recent sample  $\alpha_{old}^{(s+1)}$  and samples  $\hat{\alpha}$  from the proposal distribution. The proposed sample is accepted ( $\alpha_{new}^{(s+1)} = \hat{\alpha}$ ) with probability  $\min(1, r_\alpha)$  or rejected ( $\alpha_{new}^{(s+1)} = \alpha_{old}^{(s+1)}$ ) with probability  $1 - r_\alpha$  where the acceptance ratio,  $r_\alpha$ , is constructed as

$$r_\alpha = \frac{p(\hat{\alpha}|\beta, \eta)}{p(\alpha_{old}^{(s+1)}|\beta, \eta)} = \frac{p(\hat{\alpha})p(\eta_{old}^{(s+1)}|\hat{\alpha}, \beta_{old}^{(s+1)})}{p(\alpha_{old}^{(s+1)})p(\eta_{old}^{(s+1)}|\alpha_{old}^{(s+1)}, \beta_{old}^{(s+1)})}$$

- Sample  $\beta^{(s+1)} \sim p(\beta|\alpha^{(s+1)}, \eta^{(s)})$ : Similar procedure is followed by sampling  $\beta^{(s+1)}$  for with Metropolis algorithm till it converges. Here the acceptance ratio,  $r_\beta$ , is constructed as

$$r_\beta = \frac{p(\hat{\beta}|\alpha, \eta)}{p(\beta_{old}^{(s+1)}|\alpha, \eta)} = \frac{p(\hat{\beta}) p(\eta_{old}^{(s+1)}|\alpha_{new}^{(s+1)} \hat{\beta},)}{p(\beta_{old}^{(s+1)}) p(\eta_{old}^{(s+1)}|\alpha_{new}^{(s+1)}, \beta_{old}^{(s+1)})}$$

- Sample  $\eta^{(s+1)} \sim p(\eta|\alpha^{(s+1)}, \beta^{(s+1)}, \mathbf{y}, X)$ : As mentioned before, we employ ABC-MCMC at this stage. Similar to a typical Metropolis algorithm, we sample  $\eta^{(s+1)}$  till it converges. We propose  $\hat{\eta}$  from a proposal symmetric distribution centered at  $\eta_{old}^{(s+1)}$ . But unlike  $\alpha$  and  $\beta$ , we do not have access to an explicit expression for the likelihood  $p(\mathbf{y}, X|\eta)$ . To check the fitness of the proposed sample  $\hat{\eta}$  and to compare it with the current sample  $\eta_{old}^{(s+1)}$  without trying to find the likelihood, ABC reconstructs the acceptance ratio  $r_\eta$  as

$$r_\eta = \frac{p(\hat{\eta}|\alpha_{new}^{(s+1)}, \beta_{new}^{(s+1)})}{p(\eta_{old}^{(s+1)}|\alpha_{new}^{(s+1)}, \beta_{new}^{(s+1)})} \mathbb{I}\{d(\mathcal{S}(\hat{\mathbf{x}}), \mathcal{S}(X_o)) \geq \nu\}$$

$\mathcal{S}(\hat{\mathbf{x}})$  and  $\mathcal{S}(X_o)$  are the sufficient statistics for data nominated by  $\hat{\eta}$  and the existing data in the training set respectively,  $d(\cdot, \cdot)$  is a distance criterion between them and  $\mathbb{I}\{\cdot\}$  is an indicator function providing 0s and 1s depending on the condition passed in the parenthesis. ABC uses the distance criterion between the sufficient statistics obtained from the simulated data and the observed to accept the sampled parameter values (i.e.,  $\eta$ ). Different methods for defining the sufficient statistics have been proposed in the literature to capture the critical information in data such as nonlinearity and sparsity such as use of auxiliary model to incorporate information from the features of the entire data [53].

In the proposed work, we screen the sampled parameter values by examining their linear dependency on the training dataset to avoid redundancy and encourage generalizability. We only query the samples that maximizes the information given the already sampled data. A similar procedure has been employed for online sparsification in kernel-based nonlinear regressions, recursive least square algorithm (KRLS) [54]. We will now describe how we included the independence condition into ABC. Let us consider  $\phi$  to be the mapping of the kernel function in Hilbert space  $\mathcal{H}$  where  $\langle \phi(\mathbf{x}), \phi(\mathbf{x}') \rangle$  represents the kernel covariance matrix  $k(\mathbf{x}, \mathbf{x}')$ , according to Mercer's theorem. Here

$\langle \cdot, \cdot \rangle$  is the inner product in  $\mathcal{H}$ . The new sample  $\hat{\eta}$  proposed by Metropolis algorithm nominates a candidate data  $\hat{\mathbf{x}}$  according to Eq. (1). We consider including the sample in our list if  $\phi(\hat{\mathbf{x}})$  is approximately linearly independent from  $\phi(X_o)$  obtained from the training data. To evaluate the linear independence, we define the filtering distance  $d(\mathcal{S}(\hat{\mathbf{x}}), \mathcal{S}(X_o)) \equiv \delta$  as

$$\delta = \min_{\mathbf{a}} \left\| \sum_{i=1}^{N-1} a_i \phi(\mathbf{x}_{o_i}) - \phi(\hat{\mathbf{x}}) \right\|^2 \quad (4)$$

where  $\mathbf{a} = \{a_1, a_2, \dots, a_{N-1}\}$ . If  $\phi(\hat{\mathbf{x}}) = \sum_{i=1}^{N-1} a_i \phi(\mathbf{x}_{o_i})$ , then  $\delta = 0$  and the nominated sample  $\hat{\mathbf{x}}$  is approximately dependent of past samples. It implies that  $\hat{\mathbf{x}}$  can be inferred by the data already in the training set, and does not need a nonzero coefficient at any time. The approximate linear dependency (ALD) condition holds if  $\delta$  is below  $\nu$  which is an accuracy parameter threshold. Then  $\phi(\hat{\mathbf{x}})$  can be approximated within a squared error  $\nu$  by some linear combination of current training data. As described in [54], expanding and solving Eq. (4), we obtain

$$\mathbf{a}^* = K(X_o, X_o)^{-1} K(X_o, \hat{\mathbf{x}}) \quad \text{and} \quad \delta = K(\hat{\mathbf{x}}, \hat{\mathbf{x}}) - K(X_o, \hat{\mathbf{x}})^T \mathbf{a}^* \quad (5)$$

We consider  $\hat{\mathbf{x}}$  for inclusion only if  $\delta \geq \nu$  resulting  $\mathbb{I}\{\delta \geq \nu\} = 1$ . In that case, we compare the prior of  $\hat{\eta}$  and  $\eta_{old}^{(s+1)}$  before accepting one of them as  $\eta_{new}^{(s+1)}$ . On the other hand, if  $\delta < \nu$ , it makes  $\mathbb{I}\{\delta \geq \nu\} = 0$ , implying  $\eta_{new}^{(s+1)} = \eta_{old}^{(s+1)}$  irrespective of the priors. Authors in [54] experimented with different values for  $\nu$  using cross validation. By using extensive studies, we fixed  $\nu = 0.001$  for all our experimentation, but whether the best  $\nu$  varies for each function calls for detailed future analysis which is out of the scope of our current study.

- Let  $\boldsymbol{\theta}^{(s+1)} = \{\alpha^{(s+1)}, \beta^{(s+1)}, \eta^{(s+1)}\}$ . After generating  $\{\boldsymbol{\theta}^{(1)}, \boldsymbol{\theta}^{(2)}, \dots, \boldsymbol{\theta}^{(s)}\}$ , the approximation of  $\eta_j$  is obtained by averaging the observed  $\{\eta_j^{(1)}, \eta_j^{(2)}, \dots, \eta_j^{(s)}\}$ .

In this work, we defined the proposal distribution as  $\mathcal{N}(\boldsymbol{\theta}_{old}, \tau^2)$  where  $\boldsymbol{\theta}_{old}$  is the sample parameter accepted in the last iteration, and  $\tau^2$  is the variance designed to ensure the sample is within its allowable range [21]. The rate of convergence to target distribution depends on  $\tau$  since a too-small or too-large variance may cause the sampler to get stuck at one sample for a long time. Considering 99.7% of data following a normal distribution fall within 3 standard deviations of the mean, we calculated  $\tau^2$  each time depending on where the current mean  $\boldsymbol{\theta}_{old}$  is situated. For example,

since the allowable range of  $\eta$  is within 0 and 1, if  $\eta_{old} = 0.75$  at some stage,  $\eta_{old} + 3\tau \leq 1$  which makes  $\tau^2 \approx 0.007$ . Thus the proposal distributions were narrower when the mean was closer to its allowable boundary, and wider when close to the middle of the allowable range. We have iterated each sampling 1000 times. The steps of the entire methodology are summarized in algorithm 1.

---

**Algorithm 1:** Implementation of the algorithm with a trade-off between exploration and exploitation

---

Input:  $N$  number of training samples  $\{(\mathbf{x}_{oi}, y_{oi})\}_{i=1}^N$ ;  
 Output: Updated training set;  
**while** stopping criteria hasn't been met **do**  
     Initialize with  $\alpha^0, \beta^0, \eta^0$  ;  
     **for**  $s$  number of times **do**  
         sample  $\alpha_{new}$  with Metropolis algorithm;  
         sample  $\beta_{new}$  with Metropolis algorithm;  
         sample  $\eta_{new}$  with Metropolis algorithm with ABC;  
     **end**  
     Find  $\bar{\eta}$ , the expected value or mean of  $\eta$  from the observed samples;  
     Determine  $\mathbf{x}^*$  from Eq. (1) using  $\eta = \bar{\eta}$ ;  
     Obtain its label,  $y^*$ ;  
     Add  $(\mathbf{x}^*, y^*)$  to the training set  
**end**

---

## 3.2 Gaussian Process Regression

In the absence of any known functional form of  $f(\mathbf{x})$ , we consider Gaussian process regression (GPR) as our underlying learning model. GPR considers a distribution over the underlying function  $f(\mathbf{x})$  and aims to specify the black-box function by its mean and covariance. Due to the noise inherited in labeled data without the learner's knowledge, the output  $y$  comprises  $f(\mathbf{x})$  as

$$y = f(\mathbf{x}) + \varepsilon \quad \varepsilon \sim \mathcal{N}(\mathbf{0}, \sigma^2) \quad (6)$$

Observing the noisy outputs,  $\tilde{\mathbf{y}}$ , GPR attempts to reconstruct the underlying function  $f(\mathbf{x})$  by removing the contaminating noise  $\varepsilon$  [55]. We denote the training dataset as  $(X_o, \mathbf{y}_o)$ . GPR imposes a zero-mean Gaussian process prior over the noisy outputs such that

$$\mathbf{y}_o \sim \mathcal{N}(\mathbf{0}, K(X_o, X_o) + \sigma_n^2 I) \quad (7)$$

The joint prior distribution between the training output set  $\mathbf{y}$  and test output set  $\hat{\mathbf{f}}$  is as following

$$\begin{bmatrix} \mathbf{y} \\ \hat{\mathbf{f}} \end{bmatrix} \sim \mathcal{N}_m \left( \mathbf{0}, \begin{bmatrix} K(X_o, X_o) + \sigma_n^2 I & K(X_o, X_u) \\ K(X_u, X_o) & K(X_u, X_u) \end{bmatrix} \right) \quad (8)$$

where  $X_u$  is the set of unlabeled testing points. The posterior distribution at the test samples is given as  $\{\hat{\mathbf{f}}|X_o, \mathbf{y}_o, X_u\} \sim \mathcal{N}(\hat{\mathbf{f}}, \text{cov}(\hat{\mathbf{f}}))$ , where

$$\hat{\mathbf{f}} = K(X_u, X_o)[K(X_o, X_o) + \sigma_n^2 I]^{-1} \mathbf{y}_o \quad (9)$$

$$\text{cov}(\hat{\mathbf{f}}) = K(X_u, X_u) - K(X_u, X_o)^T [K(X_o, X_o) + \sigma_n^2 I]^{-1} K(X_o, X_u) \quad (10)$$

### 3.3 Acquisition functions

In this section, we present some of the most commonly used acquisition functions and characterize them either as an exploration or an exploitation strategy based on the literature and our extensive simulation studies.

- **Improved Greedy Sampling:** At every iteration, improved greedy sampling (iGS) determines the unexplored region by searching over the entire region in both the input and output spaces. It samples the next data which is located the farthest from its nearest training point or in an unobserved region according to the then prediction by the regression model. The acquisition function at  $\mathbf{x}_j$  is calculated as  $u(\mathbf{x}_j)v(\mathbf{x}_j)$  where  $u(\mathbf{x}_j) = \|\mathbf{x}_j - \mathbf{x}_{o_i}\|_2$ ,  $v(\mathbf{x}_j) = \|\hat{f}_j - y_{o_i}\|_2$ ,  $y_{o_i}$  = the observed output or the label at training point  $\mathbf{x}_{o_i}$ ,  $\hat{f}_j$  = the predicted output at test point  $\mathbf{x}_j$ , and  $\|\cdot\|_2$  is the L2 norm. IGS defines the distance at  $\mathbf{x}_j$  as  $u(\mathbf{x}_j)v(\mathbf{x}_j)$  instead of  $u(\mathbf{x}_j) + v(\mathbf{x}_j)$  or  $(u(\mathbf{x}_j))^2 + (v(\mathbf{x}_j))^2$  due to the possibility of significantly different scale of  $u$  and  $v$  which can hamper the latter two formulas with the dominance of one measure over another. It then selects

the next sample,  $\mathbf{x}_{\text{iGS}}^*$ , that maximizes the acquisition function as given in the following

$$\mathbf{x}_{\text{iGS}}^* = \underset{\mathbf{x}_j}{\operatorname{argmax}} \left( \min \left( \|\mathbf{x}_j - \mathbf{x}_{o_i}\|_2 \|\hat{f}_j - y_{o_i}\|_2 \right) \right) \quad (11)$$

By selecting data from unexplored regions in both input and output spaces [13], iGS avoids sampling from any concentrated region and hence satisfies the requirement for an exploration strategy.

- **Query by Committee:** Maintaining a committee of models, Query by Committee (QBC) queries the data where the committee members disagree the most about a measure of criteria. Considering a committee of  $Q$  models denoted as  $h_1, h_2, \dots, h_Q$ , we define the measure of disagreement between two models  $h_l$  and  $h_p$  at  $\mathbf{x}_j$  as the absolute difference of prediction by the respective models at that point, or  $|h_l(\mathbf{x}_j) - h_p(\mathbf{x}_j)|$ . Then the acquisition function at  $\mathbf{x}_j$  is defined as the maximum disagreement at  $\mathbf{x}_j$ , therefore,  $\max_{l,p}(|h_l(\mathbf{x}_j) - h_p(\mathbf{x}_j)|)$  where  $j = 1, 2, \dots, Q$ . Then the next data,  $\mathbf{x}_{\text{QBC}}^*$  is selected where the acquisition function is maximized following Eq. (12).

$$\mathbf{x}_{\text{QBC}}^* = \underset{\mathbf{x}_j}{\operatorname{argmax}} \left( \max_{l,p}(|h_l(\mathbf{x}_j) - h_p(\mathbf{x}_j)|) \right) \quad (12)$$

QBC approach based on GPR allows us to exploit the regions in the search space where the function's behavior is uncertain i.e., discontinuities or change points. As indicated in [55], the mean square (MS) continuity and differentiability of kernel functions control their flexibility. For example, let us compare GPR models with exponential, Matérn 3/2, Matérn 5/2, and squared exponential kernel functions. The non-differentiable exponential kernel generates the roughest prediction, whereas the infinitely differentiable squared exponential kernel produces the smoothest ones. An intermediate level of smoothness can be observed in Matérn 3/2 and Matérn 5/2 kernels which are one and two times MS differentiable respectively [55]. The sharp changes of underlying functions are captured by the rough predictions via dense queries. But the smoother prediction deviates from the underlying model at the region. Therefore, kernel functions with different MS continuity and differentiability behave differently where the functional form is unpredictable with discontinuity or sharp change. When QBC selects the data at which committee members differ the most in their prediction, it keeps exploiting that very region.

- **Maximum variance:** A learner’s expected error can be decomposed into noise, bias, and variance [8]. Since the noise is independent of the model or training data, and bias is invariant given a fixed model, minimizing the variance is intuitively guaranteed to minimize the future generalization error of the model [5]. The maximum variance strategy queries the data at each iteration where it has the highest variance predicted by the regression model. Eq. (13) provides the Gaussian process posterior covariance, and the diagonal elements of  $\text{cov}(\hat{\mathbf{f}})$  provide the predicted variance,  $\mathbb{V}$  which is the acquisition function in this strategy. The next data is queried following Eq. (13).

$$\mathbf{x}_{\text{VAR}}^* = \underset{\mathbf{x}_j}{\text{argmax}} (\mathbb{V}(\mathbf{x}_j)) \quad (13)$$

Since predicted variance is higher mostly in less-explored regions, it can be implemented as an adequate exploration acquisition function to query the next data [56].

- **Maximum entropy:** Entropy is an information-theoretic measure that often has been defined as the amount of information needed to “encode” a distribution and has been related to the uncertainty of the underlying model [5]. Thus minimizing model entropy can reasonably lead to revealing the model uncertainty. Shannon’s entropy has been used as an acquisition function named maximum entropy sampling [42] or uncertainty sampling [5]. Since the posterior prediction of the Gaussian process follows multivariate distribution, Shannon’s entropy of the distribution is

$$H[\hat{\mathbf{f}}, \text{cov}(\hat{\mathbf{f}})] = \frac{1}{2} \log |\text{cov}(\hat{\mathbf{f}})| + \frac{D}{2} \log(2\pi e)$$

where  $D$  is the dimension of the variable, and  $\hat{\mathbf{f}}$  and  $\text{cov}(\hat{\mathbf{f}})$  are the predicted mean and covariance according to Eqs. (9) and (10) respectively [55]. By minimizing the learning model uncertainty, this strategy is also more prone to exploration than exploitation. The maximum entropy strategy queries the data where it has the highest entropy following Eq.(14) as shown below.

$$\mathbf{x}_{\text{ENT}}^* = \underset{\mathbf{x}_j}{\text{argmax}} (H[\hat{\mathbf{f}}, \text{cov}(\hat{\mathbf{f}})]) \quad (14)$$

### 3.4 **Strategies for exploration-exploitation trade-off**

As touched on briefly in the introduction, the existing approaches have tried achieving the trade-off between exploration and exploitation using different methodologies. Here we have listed a few that we will compare our methodology with.

- **Static trade-off:** Many of the previous studies have held on to static trade-offs between exploration and exploitation. Prior information can be used to decide on the trade-off (e.g., equal importance to both or more importance to one based on the nature of the function). Existing approaches have conducted trial and error with different trade-off values between exploration and exploitation between appropriate exploration and exploitation acquisition functions to conduct the simulated experiments, and then select the one that promises overall better accuracy [57]. By fixing the exploration-exploitation trade-off throughout the whole learning process, this method reduces the computation complexity to a great extent. Nevertheless, the same trade-off cannot be expected to demonstrate similar performance for every function (as can be seen in the experimental results).
- **Probabilistic trade-off:** Inspired by simulated annealing [58], this algorithm updates the exploration-exploitation combination in a probabilistic approach. For instance, the exploration probability is defined as  $p_R = \alpha^{t-1}$  where  $\alpha$  is less than 1 and  $t$  is the current time step or iteration number. To query new data, a uniform random variable  $Z$  is generated, if  $Z \leq p_R$ , we consider  $\eta = 1$ , and exploration is performed, otherwise we consider  $\eta = 0$ , and exploitation is applied [18]. Hence the strategy starts with pure exploration. The exploration probability decays gradually, and the learning model gets more prone to pure exploitation over time. Intuitively, this transition is practical since the initial data queries should focus more on exploration and after learning the overall trend of the function, we can identify the irregular regions via exploitation. However, the transition rate depends on the choice of  $\alpha$  which we fixed at 0.7 following Elreedy et al. [18]. But again, the transition rate should depend on the nature of the function and fixing it will decrease the efficiency of the learning process.

## 4 Experimental results

In this section, we present the experimental setup, performance evaluation of the proposed methodology, and its comparison with other active learning strategies over six simulated experiments and one real-world case study for predicting the property of MAX phase materials.

### 4.1 Experimental setup

To demonstrate the efficacy of the proposed approach, we employ the Matérn 3/2 kernel function in the GPR model to avoid too rough (exponential kernel) or too wavy (squared exponential kernel) prediction. The kernel function is presented in Eq.(15)

$$K_{\nu=3/2}(z) = \sigma_f^2 \left(1 + \sqrt{3}z/l\right) \exp\left(-\sqrt{3}z/l\right) \quad (15)$$

where  $\sigma_f^2$  is the signal variance that we fixed at 1,  $z = \|\mathbf{x} - \mathbf{x}'\|_2$ , and  $l$  is the length-scale parameter optimized by maximizing the log marginal likelihood of the Gaussian process regression model.

While applying the QBC strategy, we maintained a committee of ten Gaussian process models, each with a different kernel function; (i) squared exponential, (ii) exponential, (iii) Matérn 3/2, (iv) Matérn 5/2, (v) rational quadratic, (vi) product of dot product and constant kernel, (vii) product of i and iii, (viii) product of i and iv, (ix) product of ii and iii, (x) product of ii and iv [55]. For the generation of the data, we fixed the signal-to-noise (SN) ratio to 10 which we define as the decibel of the ratio of signal power to the power of the data noise. For the performance evaluation, we calculated the root mean squared error as

$$\text{RMSE} = \sqrt{\sum_{k=1}^K \frac{(\hat{f}(\mathbf{x}_k) - f(\mathbf{x}_k))^2}{K}} \quad (16)$$

where  $f(\cdot)$  and  $\hat{f}(\cdot)$  represent the true and predicted response respectively. We repeated all simulated experiments 100 times to achieve a consistent estimate of the performance.

## 4.2 Simulated experiments

To demonstrate the performance of the proposed approach against the existing strategies, we considered the six following functions.

$$\bullet \quad F_1(x) = \begin{cases} 3.5 \exp\left(-\frac{(x-10)^2}{200}\right) + \epsilon, & \text{if } x \leq 25 \\ 8 - 3.5 \exp\left(-\frac{(x-35)^2}{200}\right) + \epsilon, & \text{otherwise.} \end{cases} \quad (17)$$

$$\bullet \quad F_2(x) = \sin(x) + 2 \exp(-30x^2) + \epsilon \quad x \in [-2, 2] \quad (18)$$

$$\bullet \quad F_3(x) = \sum_{i=1}^2 |x_i \sin(x_i) + 0.1x_i| + \epsilon \quad x_1, x_2 \in [-5, 5] \quad (19)$$

$$\bullet \quad F_4(x) = 2x_1^2 - 1.05x_1^4 + x_1^6/6 + x_1x_2 + x_2^2 + \epsilon \quad x_1, x_2 \in [-5, 5] \quad (20)$$

$$\bullet \quad F_5(x) = (4 - 2.1x_1^2 + x_1^4/3)x_1^2 + x_1x_2 + (4x_2^4 - 4)x_2^2 + \epsilon \quad x_1, x_2 \in [-2, 2] \quad (21)$$

$$\bullet \quad F_6(x) = \frac{1}{2} \sum_{i=1}^{10} x_i^2 - \cos(2\pi x_i) + \epsilon \quad x_i \in [-5, 5] \quad \forall i = 1, 2, \dots, 10 \quad (22)$$

First, we implement our methodology by employing iGS and QBC as the pure exploration and exploitation strategy respectively. With three random initial points in the training data, Figure 4 shows the result of iGS, QBC, and our proposed methodology after the 12<sup>th</sup> iteration for the underlying function from Eq.(18). Unsurprisingly, iGS spread out its sampled points in both  $x$  and  $y$  direction predicting the smooth portions of the function competently, but could not achieve the peak of the function due to the sudden change near  $x = 0$ . QBC exploited this uncertainty and sampled most of the points at  $x = 0$ , but ignored other regions in the process. Our methodology sampled at  $x = 0$  enough times to achieve the peak there but has also explored and provided satisfactory prediction in other regions achieving an overall lower error than the other two acquisition functions.

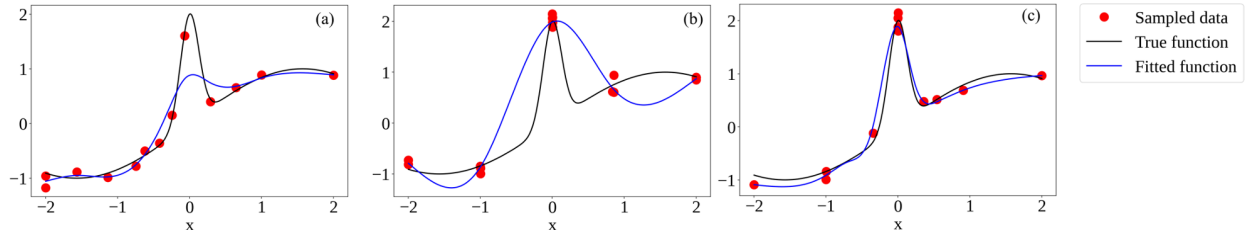


Figure 4: Sampled points and fitted function using (a) exploration, (b) exploitation, (c) proposed methodology with a dynamic trade-off between exploration and exploitation

Continuing to employ iGS and QBC as pure exploration and exploitation strategy respectively, Figure 5 (a-f) compares the root mean square error (RMSE) of different methodologies considered

in learning the underlying functions mentioned in this section and summarises the result using boxplots. For each of the examples, we have set the upper limit on the total number of experiments to be 100. The key observation in the boxplots is that our proposed methodology consistently achieves a lower generalization error with a smaller number of queried samples than any other employed strategy. Between iGS and QBC, the two acquisition functions it combines, we observe QBC to be more efficient in some cases (Figure 5(f)), and iGS in others (Figure 5(d)). Nevertheless, our approach is either better (Figure 5(d)) or at least as good as one of the approaches (Figure 5(a,f)). Eventually, it tends to converge with the result of exploration in some of the lower dimensional functions (a,b,c). But significantly lower generalization error has been obtained with the first few added data at almost every function.

Among the one-dimensional problems, in Figures 5(a,b), our proposed acquisition function clearly performed the best. After 25 iterations, maximum variance was the second-best strategy for both cases, and the proposed approach scored about 3.3% and 20% lower RMSE than maximum variance for  $F_1(x)$  (Figure 5(a)) and  $F_2(x)$  (Figure 5(b)) respectively. The consistency of lower generalization error persisted for our approach among two of the two-dimensional problems as well (Figures 5(d, e)). After adding the 25<sup>th</sup> point in  $F_3(\mathbf{x})$  (Figure 5(c)), the best two strategies were maximum variance and iGS. Our approach achieved RMSE about 6% higher than iGS, but still managed to score about 29% lower RMSE than QBC. In  $F_4(\mathbf{x})$  and  $F_5(\mathbf{x})$ , our proposed methodology surpassed others most of the time and at the 30<sup>th</sup> addition of point, achieved about 17% and 31% lower RMSE from iGS and QBC respectively which scored the closest to the proposed approach for the corresponding functions. In the ten-dimensional problem of  $F_6(\mathbf{x})$  (Figure 5(f)), the pure exploration strategy is performing better than all other acquisition functions at the 30<sup>th</sup> and 50<sup>th</sup> addition of data. Our approach still converges to pure exploration at the 75<sup>th</sup> and 100<sup>th</sup> addition and has lower RMSE from QBC at these stages. In all these cases, all active learning strategies performed better than the random sampling strategy. Our result was affected by a few decisions including our choice of kernel, sampling algorithm and proposal distribution, number of points in the initial training set, etc. However, the overall result demonstrates that our proposed approach tend to performs at least tantamount to pure exploration or pure exploitation.

Figure 6 presents the percentage improvement of our proposed strategy from the pure exploration (iGS) and pure exploitation (QBC) calculated from the average RMSE obtained in the

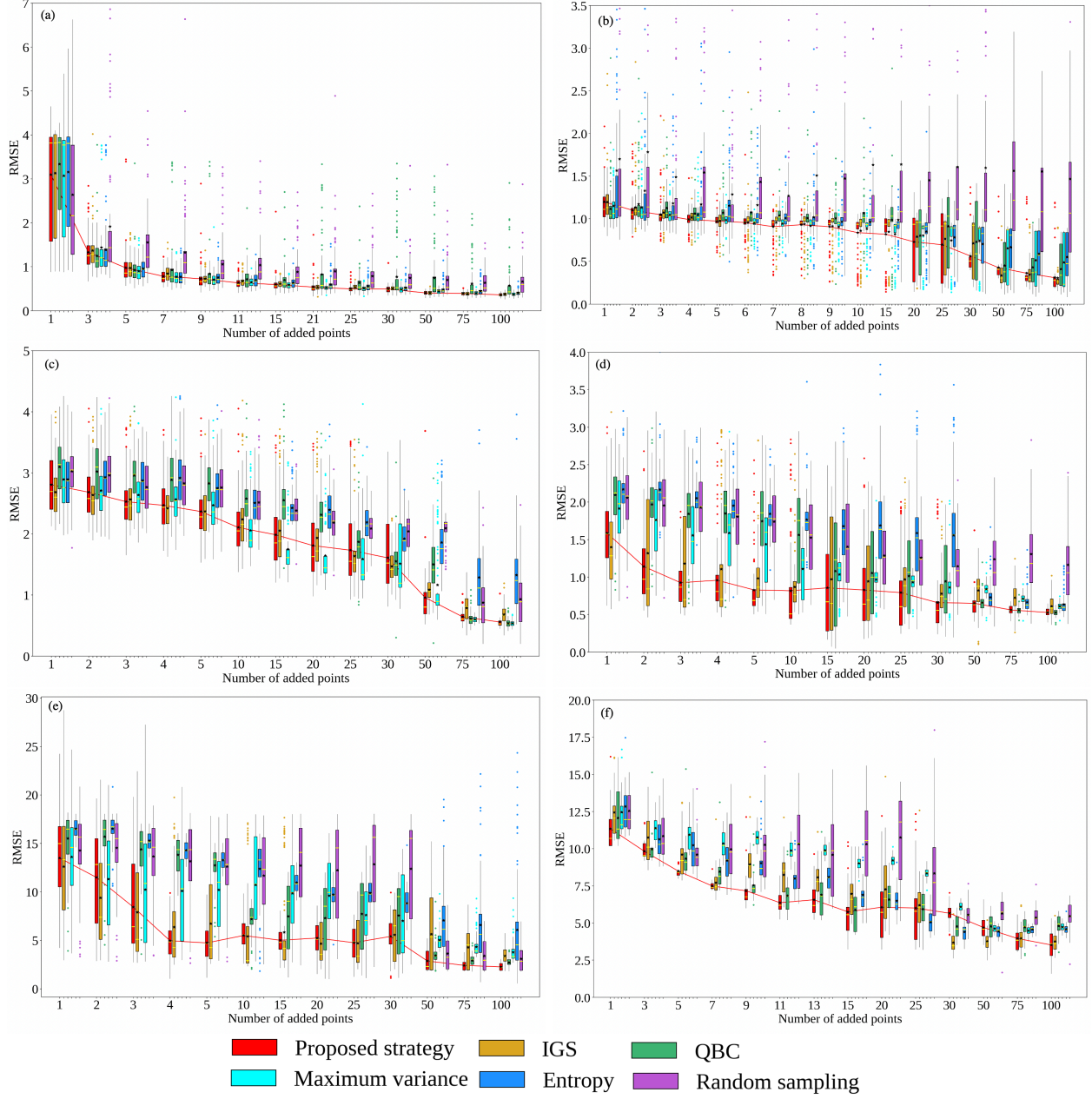


Figure 5: RMSE for proposed methodology, iGS, QBC, maximum variance, maximum entropy, and random sampling strategy for (a) Eq.(17), (b) Eq.(18), (c) Eq (19), (d) Eq (20), (e) Eq (21), (f) Eq (22)

simulated examples. Corresponding to each function, the four bars of each color represent the percentage improvement from exploration using iGS (blue) and exploitation using QBC (yellow) after the fifth, tenth, 25<sup>th</sup>, and 50<sup>th</sup> addition of data in the training set. Here, a positive and negative bar indicates improvement and deterioration of the proposed acquisition function respectively, compared to pure exploration and pure exploitation. We observe that after the 50<sup>th</sup> data inclusion,

among the forty-eight displayed results, only seven had deterioration, and the other forty-one had significant improvement and achieved lower RMSE using our proposed methodology. But more importantly, there were never two negative bars in any case, which means our approach worked better than at least one of them in all these cases.

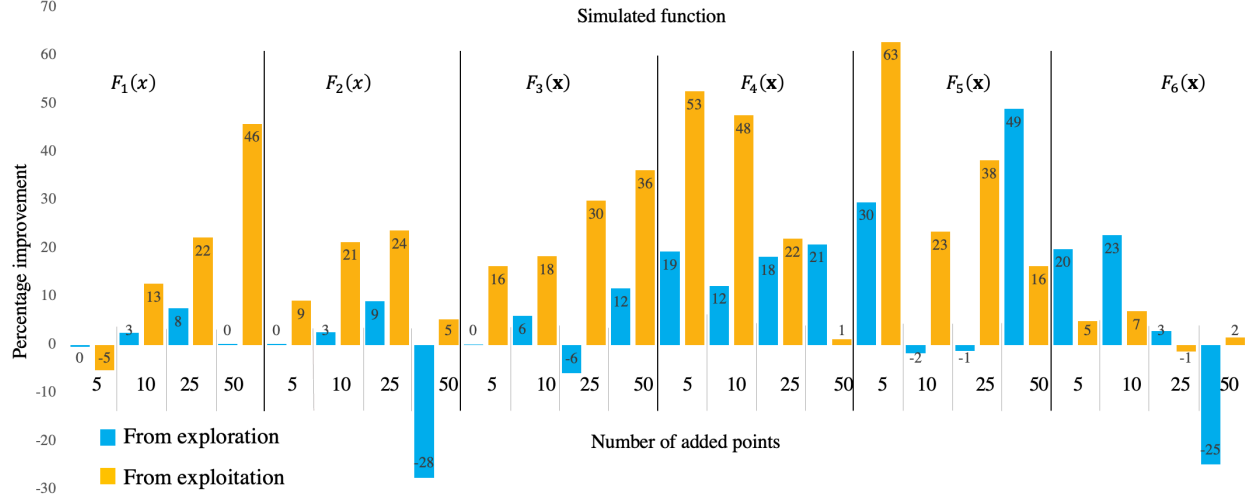


Figure 6: Percentage improvement of proposed methodology from iGS and QBC acquisition function for the six simulated studies

We also compare our proposed methodology with static and probabilistic updates of  $\eta$ . For the static trade-off, we considered  $\eta = 0.25, 0.5, 0.75$  during the learning process individually and calculated the RMSE for each of them. To note,  $\eta = 0$  and  $\eta = 1$  refer to pure exploitation and pure exploration respectively which we have already compared with our methodology in Figure 5 and Figure 6. For the probabilistic update of  $\eta$ , we followed the strategy described in Section 3.3.2. A heatmap for the average RMSE scaled for each of the comparative trade-off methodologies is presented in Table 1 where green and red cells represent more and less accurate models respectively. The heatmap clearly shows that there is no one value of  $\eta$  that works well for every function, or even for every iteration in one function. Our methodology distinctly provides better result than all the static and probabilistic trade-off.

Finally, Figure 7 presents the average improvement achieved by our strategy from pure exploration and exploitation strategy across the functions. Here, we have used iGS and maximum variance as the exploration strategy in Figure 7(a) and Figure 7(b) respectively, and QBC as the exploitation strategy in both cases. In Figure 7(a), we observe about 7% and 21% lower average

Table 1: Average RMSE for proposed methodology, static trade-off, and probabilistic trade-off after adding the 5th, 10th and 25th data for the simulated functions

Function	No. of added points	Proposed	Fixed $\eta$			Probabilistic update of $\eta$
			0.75	0.5	0.25	
$F_1$	5	0.50	0.49	0.44	0.41	0.45
	10	0.19	0.21	0.17	0.20	0.32
	25	0.00	0.05	0.04	0.06	0.36
$F_2$	5	0.26	0.24	0.24	0.27	0.33
	10	0.13	0.13	0.14	0.19	0.25
	25	0.00	0.05	0.04	0.00	0.09
$F_3$	5	0.43	0.22	0.23	0.43	0.36
	10	0.32	0.33	0.28	0.36	0.25
	25	0.16	0.04	0.00	0.14	0.02
$F_4$	5	0.02	0.20	0.22	0.59	0.49
	10	0.02	0.40	0.21	0.24	0.47
	25	0.00	0.26	0.39	0.16	0.22
$F_5$	5	0.07	0.42	0.44	0.47	0.53
	10	0.16	0.24	0.21	0.19	0.42
	25	0.08	0.07	0.00	0.15	0.19
$F_6$	5	0.27	0.27	0.30	0.33	0.33
	10	0.08	0.17	0.17	0.31	0.19
	25	0.00	0.12	0.14	0.29	0.05



RMSE from pure exploration (iGS) and exploitation (QBC) respectively. In Figure 7(b), we observe about 6% and 11% lower average RMSE from pure exploration (maximum variance) and exploitation (QBC) respectively. Overall our proposed methodology of trade-off always promises better accuracy than pure exploration and exploitation irrespective of the choice of pure strategies.

### 4.3 Case study: MAX phase materials

The layered ternary carbides and nitrides with the general formula  $M_{n+1}AX_n$  are called MAX phase materials where  $M$  and  $A$  are early transition metal and A-group elements respectively, whereas  $X$  is Nitrogen or Carbon and  $n$  is an integer between 1 and 4 [59]. Their layered structures kink and delaminate the materials during deformation resulting in an unusual and unique combination of both ceramic and metallic properties which makes them attractive candidates for structural and fuel coating applications. In this study, we intended to predict the lattice constants of MAX

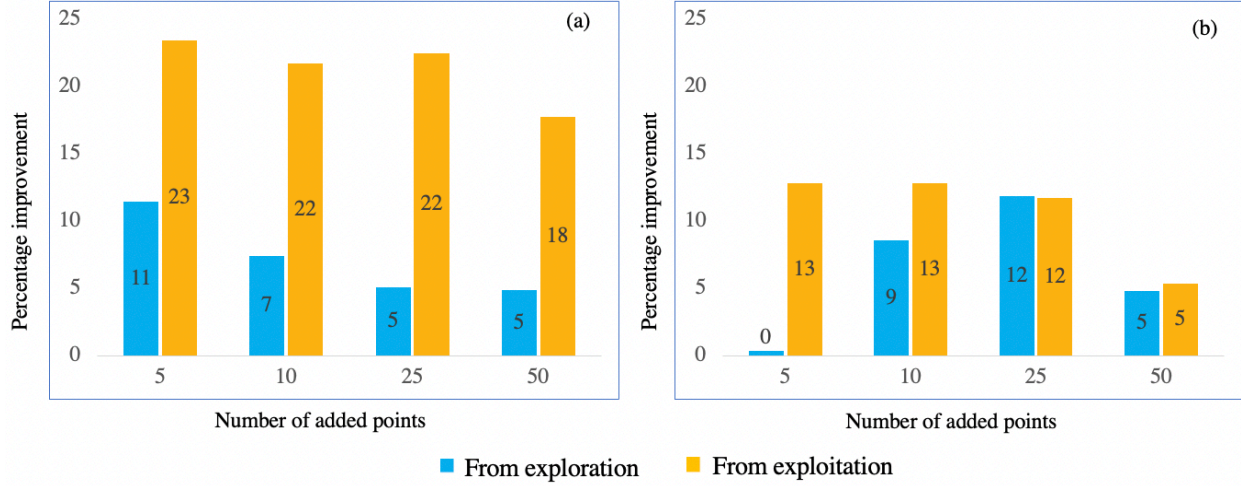


Figure 7: Average percentage improvement of proposed methodology from pure exploration ((a) iGS, (b) maximum variance) and pure exploitation (QBC) acquisition function across simulated studies

phase materials by analyzing their compositions and elastic constants using the data from Aryal et al. [60]. The lattice constant is an important piece of information to define the overall lattice structure, which helps model the microstructure evolution. To represent the discrete categorical composition features into numeric input to the models, we used one-hot encoding, a popular approach replacing the categorical variable with as many variables as categories [61]. Assuming that we wish to differentiate between two materials with the same elements in M and A, and the same value of  $n$ , one of them is a carbide, while the other is a nitride. It is possible to represent this information with two binary variables using one-hot encoding where 0 and 1 represent the non-existence and existence of that element in the material respectively.

Each category value is represented as a 2-dimensional, sparse vector of 1 for one of the dimensions, and 0 for the other. In general, for variables of cardinality  $d$ , the one-hot encoding would transfer it to  $d$  number of binary variables where each observation indicates the presence (1) or absence (0) of the dichotomous binary variable [62]. In the MAX phase problem, we have ten elements in M, twelve elements in A, and two elements in X. Hence, after using one-hot encoding and adding the numerical variable for  $n$ , we have a total of 25 variables representing the composition of the materials. Including the composition and the elastic constants, there is a total of 30 predictors to predict the lattice constant. Figure 8 provides a comparative analysis of RMSE of different methodologies employed in this case study. Our proposed methodology (combining iGS and QBC)

outperformed the other strategies and surpassed at least one of the pure exploration or exploitation in almost every iteration. Our methodology achieved about 6.4% and 8.8% average improvement from the pure exploration and exploitation strategy respectively.

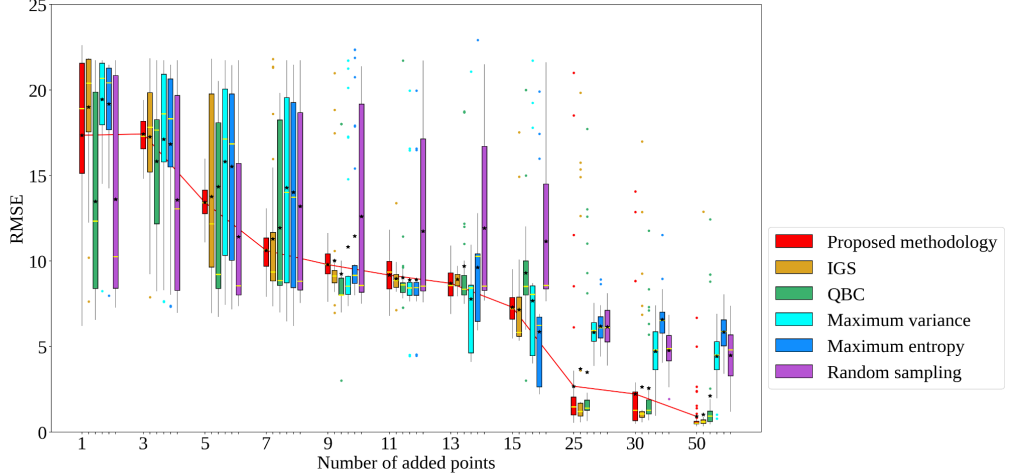


Figure 8: Comparison of RMSE for different strategies for Max phase material case study

## 5 Conclusion

In this work, we acknowledged the exploration-exploitation dilemma in active learning for regression problems. We presented a methodology using the Bayesian hierarchical model for dynamic trade-off between exploration and exploitation during active learning in the regression setting. In the hierarchical model, we presented a new approach for approximate Bayesian computation using the linear dependence of data samples in high dimensional feature space obtained via kernel trick. We demonstrated and compared our methodology with exploration, exploitation, and other well-known strategies in the simulated and real-world case studies. From the average percentage improvement in the six simulated experiments, the proposed acquisition function achieved at least 6% and 11% lower average RMSE from exploration and exploitation respectively irrespective of the chosen pure strategies. Overall, when compared to existing active learning approaches, our proposed methodology converged with fewer iterations in all cases and performed better or at least as good as the more efficient strategy among the two strategies it combines. The proposed approach to dynamically balancing exploration and exploitation has wide applications in various domains where

conducting experiments and labeling data is costly such as materials characterization, mechanical testing, manufacturing, and medical sciences.

Some of the limitations of the current studies include the assumption on the filtering distance threshold  $\nu$  and more importantly, a restricted prior on the trade-off parameter  $\eta$ . In future works, we plan to consider a more expressive and flexible Dirichlet process prior to ensure consistency and faster convergence of the hierarchical model, and also consider another hierarchy to include the  $\nu$  parameter in the model.

## References

- [1] T. Lookman *et al.*, “Active learning in materials science with emphasis on adaptive sampling using uncertainties for targeted design,” *npj Computational Materials*, vol. 5, no. 1, pp. 2057–3960, 2019.
- [2] T. Wuest *et al.*, “Machine learning in manufacturing: Advantages, challenges, and applications,” *Production & Manufacturing Research*, vol. 4, no. 1, pp. 23–45, 2016.
- [3] D. S. Char, N. H. Shah, and D. Magnus, “Implementing machine learning in health care—addressing ethical challenges,” *The New England journal of medicine*, vol. 378, no. 11, p. 981, 2018.
- [4] T. W. Liao and G. Li, “Metaheuristic-based inverse design of materials – A survey,” *Journal of Materomics*, vol. 6, no. 2, pp. 414–430, Jun. 2020, ISSN: 2352-8478. DOI: 10.1016/j.jmat.2020.02.011.
- [5] B. Settles, “Active learning literature survey,” University of Wisconsin–Madison, Computer Sciences Technical Report 1648, 2009.
- [6] D. Angluin, “Queries and concept learning,” *Machine Learning*, vol. 2, no. 4, pp. 319–342, 1988.
- [7] D. D. Lewis and W. A. Gale, “A sequential algorithm for training text classifiers,” in *SI-GIR’94*, Springer, 1994, pp. 3–12.
- [8] D. A. Cohn, Z. Ghahramani, and M. I. Jordan, “Active learning with statistical models,” *Journal of Artificial Intelligence Research*, vol. 4, pp. 129–145, 1996.
- [9] D. D. Lewis and J. Catlett, “Heterogeneous uncertainty sampling for supervised learning,” in *Machine Learning Proceedings 1994*, Elsevier, 1994, pp. 148–156.
- [10] D. J. MacKay, “Information-based objective functions for active data selection,” *Neural Computation*, vol. 4, no. 4, pp. 590–604, 1992.
- [11] J. Močkus, “On bayesian methods for seeking the extremum,” in *Optimization Techniques IFIP Technical Conference*, Springer, 1975, pp. 400–404.
- [12] N. Cebron and M. R. Berthold, “Active learning for object classification: From exploration to exploitation,” *Data Mining and Knowledge Discovery*, vol. 18, pp. 283–299, 2009.
- [13] D. Wu, C.-T. Lin, and J. Huang, “Active learning for regression using greedy sampling,” *Information Sciences*, vol. 474, pp. 90–105, 2019.
- [14] R. Burbidge, J. J. Rowland, and R. D. King, “Active learning for regression based on query by committee,” in *Lecture Notes in Computer Science*, Berlin, Heidelberg, 2007.

[15] D. R. Jones, M. Schonlau, and W. J. Welch, “Efficient Global Optimization of Expensive Black-Box Functions,” *Journal of Global Optimization*, vol. 13, no. 4, pp. 455–492, Dec. 1998, ISSN: 1573-2916. DOI: 10.1023/A:1008306431147.

[16] Z. Chen, S. Mak, and C. F. J. Wu, *A hierarchical expected improvement method for bayesian optimization*. [Online]. Available: [arXiv:1911.07285](https://arxiv.org/abs/1911.07285).

[17] A. Ajdari and H. Mahlooji, “An adaptive exploration-exploitation algorithm for constructing metamodels in random simulation using a novel sequential experimental design,” *Communications in Statistics - Simulation and Computation*, vol. 43, no. 5, pp. 947–968, 2014.

[18] D. Elreedy, A. F. Atiya, and S. I. Shaheen, “A novel active learning regression framework for balancing the exploration-exploitation trade-off,” *Entropy*, vol. 21, no. 7, 2019.

[19] N. Srinivas *et al.*, “Gaussian process optimization in the bandit setting: No regret and experimental design,” *arXiv preprint arXiv:0912.3995*, 2009.

[20] H. Afifi and H. Karl, “Reinforcement learning for virtual network embedding in wireless sensor networks,” in *2020 16th International Conference on Wireless and Mobile Computing, Networking and Communications (WiMob)(50308)*, IEEE, 2020, pp. 123–128.

[21] A. Gelman *et al.*, *Bayesian data analysis*. Chapman and Hall/CRC, 1995.

[22] F. Guo, D. K. Dey, and K. E. Holsinger, “A bayesian hierarchical model for analysis of single-nucleotide polymorphisms diversity in multilocus, multipopulation samples,” *Journal of the American Statistical Association*, vol. 104, no. 485, pp. 142–154, 2009.

[23] R. A. Fisher, “Design of experiments,” *British Medical Journal*, vol. 1, no. 3923, p. 554, 1936.

[24] H. Chernoff, “Sequential design of experiments,” *The Annals of Mathematical Statistics*, vol. 30, no. 3, pp. 755–770, 1959.

[25] W. J. Blot and D. A. Meeter, “Sequential experimental design procedures,” *Journal of the American Statistical Association*, vol. 68, no. 343, pp. 586–593, 1973.

[26] K. Yu, J. Bi, and V. Tresp, “Active learning via transductive experimental design,” in *Proceedings of the 23rd International Conference on Machine Learning*, 2006, pp. 1081–1088.

[27] C. E. Shannon, *A mathematical theory of communication*. The Bell system technical journal, 1948.

[28] N. Roy and A. McCallum, “Toward optimal active learning through sampling estimation of error reduction,” in *ICML*, 2001.

[29] R. Meka *et al.*, “An active learning methodology for efficient estimation of expensive noisy black-box functions using gaussian process regression,” *IEEE Access*, vol. 8, pp. 111 460–111 474, 2020.

[30] H. S. Seung, M. Opper, and H. Sompolinsky, “Query by committee,” in *Proceedings of the fifth annual workshop on Computational learning theory*, New York, NY, USA: Association for Computing Machinery, Jul. 1992, pp. 287–294. DOI: 10.1145/130385.130417.

[31] I. Dagan and S. P. Engelson, “Committee-based sampling for training probabilistic classifiers,” in *Machine Learning 1995*, Elsevier, 1995, pp. 150–157.

[32] K. Nigam and A. McCallum, “Pool-based active learning for text classification,” in *Conference on Automated Learning and Discovery (CONALD)*, 1998.

[33] A. Krogh and J. Vedelsby, “Neural network ensembles, cross validation, and active learning,” *Advances in Neural Information Processing Systems*, vol. 7, no. 7, 1995.

[34] T. RayChaudhuri and L. G. Hamey, “Minimisation of data collection by active learning,” in *Proceedings of ICNN’95-International Conference on Neural Networks*, vol. 3, IEEE, 1995.

[35] N. Abe and H. Mamitsuka, “Query learning strategies using boosting and bagging,” in *Proceedings of the Fifteenth International Conference on Machine Learning*, 1998, pp. 1–9.

[36] B. Settles and M. Craven, “An analysis of active learning strategies for sequence labeling tasks,” in *Proceedings of the 2008 Conference on Empirical Methods in Natural Language Processing*, 2008, pp. 1070–1079.

[37] W. Cai, Y. Zhang, and J. Zhou, “Maximizing expected model change for active learning in regression,” in *2013 IEEE 13th International Conference on Data Mining*, IEEE, 2013.

[38] J. O’Neill, S. J. Delany, and B. MacNamee, “Model-free and model-based active learning for regression,” in *Advances in Computational Intelligence Systems*, Springer, 2017, pp. 375–386.

[39] R. Hu, S. J. Delany, and B. M. Namee, “Egal: Exploration guided active learning for tcbr,” in *International Conference on Case-Based Reasoning*, Springer, 2010, pp. 156–170.

[40] H. Yu and S. Kim, “Passive Sampling for Regression,” in *2010 IEEE International Conference on Data Mining*, IEEE, Dec. 2010, pp. 1151–1156. DOI: 10.1109/ICDM.2010.9.

[41] Y. Baram, R. E. Yaniv, and K. Luz, “Online choice of active learning algorithms,” *Journal of Machine Learning Research*, vol. 5, no. Mar, pp. 255–291, 2004.

[42] A. Holub, P. Perona, and M. C. Burl, “Entropy-based active learning for object recognition,” in *2008 IEEE Computer Society Conference on Computer Vision and Pattern Recognition Workshops*, IEEE, 2008, pp. 1–8.

[43] T. Osugi, D. Kim, and S. Scott, “Balancing exploration and exploitation: A new algorithm for active machine learning,” in *Fifth IEEE International Conference on Data Mining (ICDM’05)*, IEEE, 2005.

[44] C. Yin *et al.*, “Deep similarity-based batch mode active learning with exploration-exploitation,” in *2017 IEEE International Conference on Data Mining (ICDM)*, IEEE, 2017, pp. 575–584.

[45] J. D. Cohen, S. M. McClure, and J. Y. Angela, “Should i stay or should i go? how the human brain manages,”

[46] P. A. Rabbitt, “Errors and error correction in choice-response tasks.,” *Journal of Experimental Psychology*, vol. 71, no. 2, p. 264, 1966.

[47] J. M. Bernardo, “The concept of exchangeability and its applications,” *Far East Journal of Mathematical Sciences*, vol. 4, pp. 111–122, 1996.

[48] P. D. Hoff, *A first course in Bayesian statistical methods*. Springer, 2009, vol. 580.

[49] A. G. Busetto and J. M. Buhmann, “Stable bayesian parameter estimation for biological dynamical systems,” in *2009 International Conference on Computational Science and Engineering*, IEEE, vol. 1, 2009, pp. 148–157.

[50] J. K. Pritchard *et al.*, “Population growth of human y chromosomes: A study of y chromosome microsatellites.,” *Molecular Biology and Evolution*, vol. 16, no. 12, pp. 1791–1798, 1999.

[51] P. Marjoram *et al.*, “Markov chain monte carlo without likelihoods,” *Proceedings of the National Academy of Sciences*, vol. 100, no. 26, pp. 15 324–15 328, 2003.

[52] A. E. Gelfand, “Gibbs sampling,” *Journal of the American statistical Association*, vol. 95, no. 452, pp. 1300–1304, 2000.

- [53] G. M. Martin *et al.*, “Auxiliary likelihood-based approximate bayesian computation in state space models,” *Journal of Computational and Graphical Statistics*, vol. 28, no. 3, pp. 508–522, 2019.
- [54] Y. Engel, S. Mannor, and R. Meir, “The kernel recursive least-squares algorithm,” *IEEE Transactions on Signal Processing*, vol. 52, no. 8, pp. 2275–2285, 2004.
- [55] C. K. Williams and C. E. Rasmussen, *Gaussian Processes for Machine Learning*. The MIT Press, 2006.
- [56] Y. Yang and M. Loog, “A variance maximization criterion for active learning,” *Pattern Recognition*, vol. 78, pp. 358–370, 2018.
- [57] M. P. Lourenço *et al.*, “A new active learning approach for adsorbate–substrate structural elucidation in silico,” *Journal of Molecular Modeling*, vol. 28, no. 6, pp. 1–11, 2022.
- [58] P. J. Van Laarhoven and E. H. Aarts, “Simulated annealing,” in *Simulated annealing: Theory and applications*, Springer, 1987, pp. 7–15.
- [59] P. Eklund *et al.*, “Homoepitaxial growth of ti–si–c max-phase thin films on bulk Ti<sub>3</sub>SiC<sub>2</sub> substrates,” *Journal of Crystal Growth*, vol. 304, no. 1, pp. 264–269, 2007.
- [60] S. Aryal *et al.*, “A genomic approach to the stability, elastic, and electronic properties of the max phases,” *Physica Status Solidi (b)*, vol. 251, no. 8, pp. 1480–1497, 2014.
- [61] E. C. Garrido-Merchán and D. Hernández-Lobato, “Dealing with categorical and integer-valued variables in bayesian optimization with gaussian processes,” *Neurocomputing*, vol. 380, pp. 20–35, 2020.
- [62] K. Potdar, T. S. Pardawala, and C. D. Pai, “A comparative study of categorical variable encoding techniques for neural network classifiers,” *International Journal of Computer Applications*, vol. 175, no. 4, pp. 7–9, 2017.